JOURNAL OF GUIDANCE, CONTROL, AND DYNAMICS
Vol. 18, No. 6, November–December 1995

Nonlinear Control Law for Aerial Towed Target

Alexander S. Bourmistrov, Robin D. Hill, and Paul Riseborough
Royal Melbourne Institute of Technology, Melbourne, Victoria 3001, Australia

The control law for a maneuverable towed target is derived using inversion of nonlinear dynamic and kinematic equations of motion that take the cable tension force into account. Dynamic properties of the states allowed for construction of lower order subsystems with different time scales for their variables. These faster and slower parts were inverted consecutively to control flight-path angles of the towed vehicle. A procedure is described for estimation of the aerodynamic and tension forces acting on the target and states unavailable for direct measurements from a conventional set of feedback parameters. Guidance and station-keeping properties of the control law are demonstrated by simulation results.

Nomenclature

$Cx_by_bz_b$	= target body-fixed coordinate system
I_x, I_y, I_z	= moments of inertia about body axis
L, D, Y	= aerodynamic lift, drag, and side force on the target
l_a, m_a, n_a	= aerodynamic rolling, pitching, and yawing moment
M	= target mass
$Oxyz$	= local vertical inertial coordinate system with origin at the center of mass of the target trimmed with controls locked
p, q, r	= body axis roll, pitch, and yaw rate
$\bar{q}$	= aerodynamic pressure
T_x, T_y, T_z	= body axis components of cable tension force
u, v, w	= body axis velocity components
V	= target velocity
x, y, z	= inertial coordinates of the center of mass of the target
α	= angle of attack, $\tan^{-1}(w/u)$
β	= sideslip angle, $\sin^{-1}(v/V)$
$\delta_A, \delta_E, \delta_R$	= ailerons, elevator, and rudder deflection angles
ϕ, θ, ψ	= Euler angles
χ, γ	= horizontal and vertical flight-path angles

Subscripts

c	= commanded
d	= desired

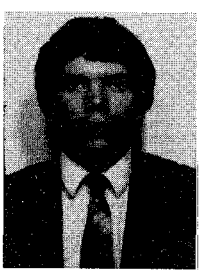

Alexander S. Bourmistrov received his B.S. degree from the Moscow Aviation Institute, Faculty of Cosmonautics and Automated Spacecrafts, Department of Dynamics and Flight Control, in 1986. From 1986 to 1992 he was a research engineer with the Institute of Control Sciences, Russian Academy of Sciences, Moscow. In 1993, he joined the Department of Aerospace Engineering at the Royal Melbourne Institute of Technology, where he is currently continuing research as a doctoral student. His theoretical research interests include time-domain signal shaping in linear feedback systems and nonlinear robust control.

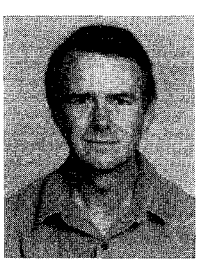

Robin D. Hill was born in Bombay, India, in 1950. He received the B.Sc. and Ph.D. degrees from Monash University, Australia, in 1972 and 1978, respectively. He held a Humboldt Postdoctoral Fellowship at the Technical University of Munich, 1979–1980. From 1982 to 1990 he was a research scientist in the Australian Defence Science and Technology Organisation, working mainly on control of airborne vehicles. Since 1990 he has been with the Department of Mathematics, Royal Melbourne Institute of Technology, currently as Senior Lecturer. His research interests are in the applications of optimization theory to engineering problems.

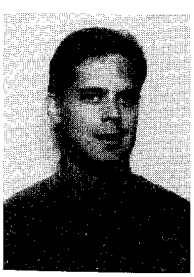

Paul Riseborough received his B.Eng. degree in 1990 and Ph.D. degree in 1994 from the Royal Melbourne Institute of Technology (RMIT), Department of Aerospace Engineering. He has taught a course Dynamics and Control of Flight for undergraduate students. He currently works for the Sir Lawrence Wackett Centre for Aerospace Design Technology at RMIT as a Research Associate funded by the Australian Research Council. His research interests include l_1-optimal control of smart structures and nonlinear robust control.

Received June 22, 1994; revision received Feb. 20, 1995; accepted for publication March 22, 1995.

Introduction

A MANEUVERABLE aerial towed target capable of evaluating a set of prescribed maneuvers is effective in a number of engineering applications. The guidance control system of the target is considered to be functioning independently of the tow aircraft except for the cable constraints.

Reference 1 presents the design of a control system for a towed vehicle that combines autopilots for stability augmentation, transferring the vehicle from one trim position into another and station keeping. The suggested guidance algorithm assumes availability of tables of a priori estimates for required control surface deflections at a particular trim point. The classical approach of Ref. 1 has been successfully flight tested. However, linearizing assumptions and neglect of the cable tension force restrict the flight envelope of the towed system and may result in reduced performance in rapid maneuvering of the target.

The design of the control law in this paper is based on a nonlinear inversion (NI) technique that follows from general decoupling theory applied over recent years to a class of nonlinear systems.[2–4] The fact that the control vector can be extracted from the basic nonlinear system representation allows for derivation of control laws simply by inverting the system dynamic and kinematic equations of motion. A six degree-of-freedom model of the towed target that takes the cable tension force and spatial dependence into account was employed to synthesize the autonomous control system for generation and tracking of the three-dimensional trajectories. The different time scale properties of the states allowed for order reduction of the basic nonlinear system. A dramatic effect of this technique was recognized in feedback control design for nonlinear systems.[5–7] Reference 6 gives examples of feedback control laws and stability analysis for a class of nonlinear systems with different time scales for the state variables. References 5 and 7 present the control designs for an aircraft that were developed using the inversion of the dynamic and kinematic equations of motion. These designs demonstrate significant performance improvements over conventional control systems and enable controllable flight in highly nonlinear regions of the flight envelope.

To simulate six degree-of-freedom motion of the towed system, a discrete model of the cable, referred to as a point mass model, was developed assuming the cable to be flexible and inextensible. References 1 and 8–10 discuss different approaches to mathematical modeling of the tow cable. The cable model governing differential equations and the boundary conditions, which were used in this study, were solved using the variable step Kutta–Merson integration routine for simulation of the towed system motion. The towed system configuration and dynamic properties of the developed point-mass model in the considered flight regimes were compared with computationally expensive cable simulators[11,12] and showed satisfactory performance matching. The results of the closed-loop simulation with the NI control laws developed in this paper are presented.

For the purposes of this paper the towing aircraft was assumed to be in straight and level flight with a constant speed. With this assumption, it was found convenient to place the origin of the inertial reference frame at the center of mass of the towed target trimmed with aerodynamic controls locked.

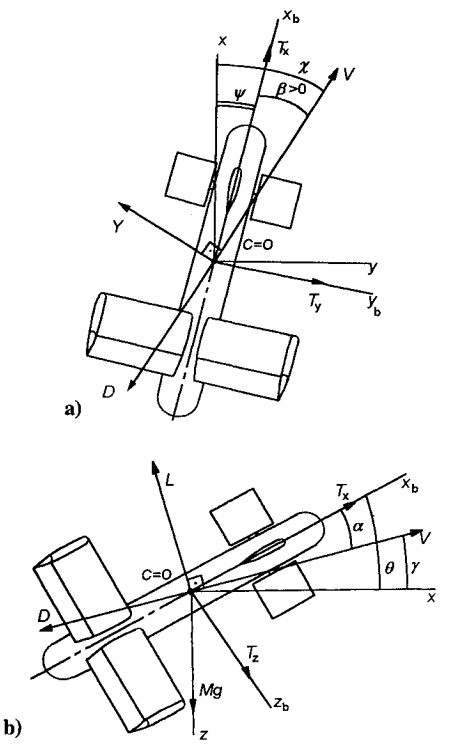

Fig. 1 Vector geometry in a) horizontal and b) vertical planes.

Towed Target Model

The following aspects were accounted for in the choice of equations and analysis of the target dynamics. Firstly, the geometry of the vehicle results in a moment of inertia about the x_b body axis much smaller than that about the y_b and z_b body axes. This fact makes the coupling between the lateral and longitudinal equations significant and can be easily seen by examining the basic rigid-body moment equations. Secondly, the presence of the cable tension force couples the motion of the towed body in horizontal and vertical directions. The target attitude, as well as the position of its center of mass relative to the aircraft, determines the magnitude and orientation of the tension force and thus necessitates inclusion of spatial dependence into the system dynamics. Finally, due to vehicle symmetry and the distribution of the cable-target system forces, side motion is affected by sideslip angle to an even larger extent than vertical motion by changing angle of attack.

A schematic configuration of the towed target and the vector geometry adopted is shown in Figs. 1a and 1b for horizontal and vertical planes, respectively. Available aerodynamic controls are forward canards for pitch and yaw control and ailerons for roll control. The tension force of the tow cable is represented by its body axis components. The target's six degree-of-freedom equations of motion used to derive the nonlinear control law are given next. These are 12 first-order, nonlinear, differential equations:

$$\begin{bmatrix} \dot{p} \\ \dot{q} \\ \dot{r} \end{bmatrix} = \begin{bmatrix} 0 \\ (I_z - I_x)/I_y \cdot pr \\ (I_x - I_y)/I_z \cdot pq \end{bmatrix} + \begin{bmatrix} l_a \\ m_a \\ n_a \end{bmatrix} \tag{1–3}$$

$$\begin{bmatrix} \dot{\beta} \\ \dot{\alpha} \\ \dot{\phi} \end{bmatrix} = \begin{bmatrix} \sin\alpha & 0 & -\cos\alpha \\ -\tan\beta\cos\alpha & 1 & -\tan\beta\sin\alpha \\ 1 & 0 & 0 \end{bmatrix} \begin{bmatrix} p \\ q \\ r \end{bmatrix} + \begin{bmatrix} \dot{\chi}\cos\gamma \\ -\dot{\gamma}\sec\beta \\ 0 \end{bmatrix} \tag{4–6}$$

$$\begin{bmatrix} \dot{V} \\ \dot{\chi} \\ \dot{\gamma} \end{bmatrix} = \begin{bmatrix} (-D + T_y\cos\alpha\sin\beta + T_x\cos\beta\cos\alpha + T_z\cos\beta\sin\alpha)/M - g\sin\gamma \\ \sec\gamma(Y + T_y\cos\beta - T_x\sin\beta\cos\alpha - T_z\sin\beta\sin\alpha)/(MV) \\ (L + T_x\sin\alpha - T_y\sin\alpha\sin\beta - T_z\cos\alpha)/(MV) - g\cos\gamma/V \end{bmatrix} \tag{7–9}$$

$$\begin{bmatrix} \dot{x} \\ \dot{y} \\ \dot{z} \end{bmatrix} \begin{bmatrix} V\cos\gamma\cos\chi \\ V\cos\gamma\sin\chi \\ V\sin\gamma \end{bmatrix} \tag{10–12}$$

The states p, q, and r are governed by Eqs. (1–3), which are derived from the Euler equations. They assume symmetry of the

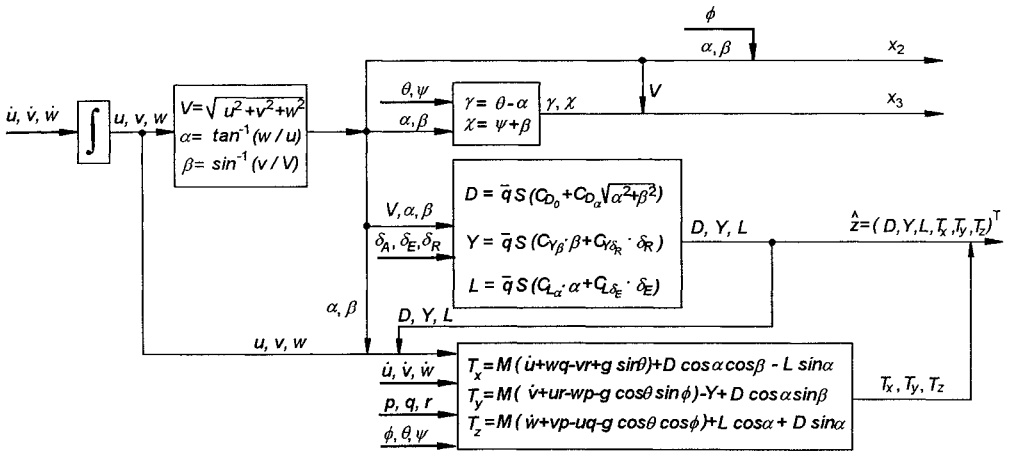

Fig. 2 Block diagram of the feedback state estimation procedure.

target about the $x_b z_b$ and $x_b y_b$ planes (i.e., inertia products are zero) and attachment of the cable to the center of gravity of the target; hence, no angular moment from the cable is produced.

Equations (4–6) govern the angles β, α, and ϕ. The first two equations are obtained[5] by resolving forces into the body axis directions to give $\dot{u}$, $\dot{v}$, and $\dot{w}$, which are related to $\dot{\alpha}$ and $\dot{\beta}$ through the relationships $\alpha = \tan^{-1}(w/u)$ and $\beta = \sin^{-1}(v/V)$. Equation (6) is one of the simplified kinematic equations that connect components of the angular velocity in the inertial axis and body axis systems.

Equations (7–9) govern the magnitude and direction of the velocity vector. They are derived by considering the target as a point mass and resolving all of the forces acting on the target into three directions. The component in the direction of the velocity vector gives $M\dot{V}$, the component in the upward-pointing normal to V within the vertical plane gives $MV\dot{\gamma}$ and the horizontal normal to V gives $MV\dot{\chi}\cos\gamma$.

Equations (4–9) are given for zero bank angle. It will be shown that this simplification is reasonable for target maneuvering motion when zero roll angle is commanded, as the ailerons can track this command very effectively. Equations (10–12) constitute the relation of the displacement of the target center of mass in the inertial reference frame with the magnitude and direction of the velocity vector. These are used to generate three-dimensional trajectories for the towed target.

Feedback State Estimator

Most of the variables included in the state vector are not available directly from measurements. However, their estimates can be obtained from a conventional feedback set. The measurable parameters assumed are body axis linear accelerations $\dot{u}$, $\dot{v}$, $\dot{w}$, angular rates p, q, r, and the Euler angles ϕ, θ, ψ, which specify orientation of the body axis system with respect to the inertial axis system. The right-hand sides of Eqs. (7–9) include aerodynamic forces and body axes components of the tension force. It is assumed that the cable attachment device is able to rotate freely around the longitudinal axis of the target with the cable attached through a gimbal joint to the target's center of mass. With such design the tension magnitude and its orientation relative to the target body axis could be measured by means of a strain gauge and two potentiometers. A procedure that was used in simulation for estimation of the forces acting on the target and states unavailable through direct measurements is described later. Body axis velocity components u, v, w, obtained by integrating the measurable accelerations, were used to estimate the target velocity magnitude, sideslip angle, and angle of attack. These angle estimates together with Euler angles give horizontal and vertical flight-path angles through the geometric relations shown in Fig. 1. It should be mentioned that high sensitivity of the estimates to integration and accelerometer errors permits use of this procedure only within relatively small operational time intervals. Otherwise, a method of periodical correction of the velocity components should be provided.

Aerodynamic forces D, Y, and L are assumed to be functions of the states V, α, and β and of the vector of control deflections $u = [\delta_A, \delta_E, \delta_R]^T$. The commanded values of the controls are used in the estimation procedure. The actuator time constants of the towed vehicle are assumed to be small enough not to cause any significant performance degradation; thus actuator dynamics are neglected in obtaining the estimates of the forces. In some other investigations into nonlinear flight control design, such as Ref. 13, for example, actuator state equations are taken into account in the design of the control law.

Well-known equations of motion of an aerial rigid body were employed to obtain the body axis components of the tension force T_x, T_y, and T_z. The block diagram of the complete estimation procedure is shown in Fig. 2.

The vector of the estimated forces $\hat{z}$ is used as an input parameter vector for the control system synthesized to guide the target motion.

Feedback Control Law for Towed Target

The system of Eqs. (1–12) can be written in a general form as follows:

$$\dot{x} = F(x, u) \tag{13}$$

where

$$x = \begin{bmatrix} x_1 \\ x_2 \\ x_3 \\ x_4 \end{bmatrix} = \begin{bmatrix} (p, q, r)^T \\ (\beta, \alpha, \phi)^T \\ (V, \chi, \gamma)^T \\ (x, y, z)^T \end{bmatrix}, \qquad u = \begin{bmatrix} \delta_A \\ \delta_E \\ \delta_R \end{bmatrix} \tag{14}$$

Equation (13) can be stated explicitly only if the model of the tow cable and the aerodynamic model (either functional or table lookup) of the target are provided to determine aerodynamic and tension force contributions.

The general decoupling theory was developed for nonlinear, time-variable parameter systems[2–4] where the number of independently controlled outputs is not larger than the dimension of the available control vector. Thus, direct application of the method to the towed target control design is not possible because the number of aerodynamic controls is not sufficient to decouple and control six degree-of-freedom motion of the target. To circumvent this difficulty in other applications researchers have used the two-time-scale properties of the dynamic states for decomposition of the basic nonlinear system into separate lower order subsystems in feedback control designs.[5–7] The simulation results presented here show that there is a significant difference in the time scales between the fast and slow states in the model of the target, and thus the use of this approach can be justified.

For the design in this paper, the fast dynamics correspond to the states p, q, and r, which are controlled by aileron, rudder, and elevator inputs. Desired moments are calculated based on the rigid-body moment equations of motion. Body attitudes relative to the airflow are then controlled with the three angular rate commands. These state variables represent slow dynamics for this design. Desired angular rates are calculated based on kinematic equations to control

roll angle, sideslip angle, and angle of attack. The target velocity vector direction, i.e., heading and flight-path angles, is controlled using target attitude commands. Desired attitude of the target relative to the airflow is calculated based on point mass equations of motion.

The major assumption made in derivation of the control law for the slower states is that the transients of the faster states decay to their commanded values quickly enough to have a negligible effect on the slower states.

With this selection of state variables and their separation into fast and slow, the target dynamics can be represented as shown in Fig. 3. Dynamic blocks are written in a form convenient for direct application of the inversion. The matrices g_i and h_i are nonlinear functions of the states provided either through direct feedback or by a feedback state estimator. The form of the matrices is discussed further later.

Employing the linear aerodynamic model of the target used in Ref. 1, Eqs. (1–3) can be written as

$$\dot{x}_1 = g_1(x) + h_1(x) \cdot u \tag{15}$$

where

$$g_1(x) = \begin{bmatrix} \bar{q}S_b^2 C_{lp}/(2VI_x)p \\ (I_z - I_x)/I_y pr + \bar{q}Sc/I_y(C_{m\alpha}\alpha + c/(2V)C_{mq}q) \\ (I_x - I_y)/I_z pq + \bar{q}Sc/I_z(C_{n\beta}\beta + c/(2V)C_{nr}r) \end{bmatrix}$$

$$h_1(x) = \begin{bmatrix} \bar{q}SbC_{l\delta_A}/I_x & 0 & 0 \\ 0 & \bar{q}ScC_{m\delta_R}/I_y & 0 \\ 0 & 0 & \bar{q}ScC_{n\delta_R}/I_z \end{bmatrix}$$

More sophisticated models can be used to describe aerodynamics of the vehicle. Reference 4 discusses application of bicubic spline interpolation over the nonlinear space of actual aerodynamic data in the feedback control law. As a next step, Eq. (15) is inverted to yield the control vector u necessary to produce desired angular accelerations, which are specified in this design by the following feedback dynamics:

$$\dot{x}_{1d} = B_1[x_{1c} - x_1] \tag{16}$$

where x_1 is the vector of measured roll, pitch, and yaw rates provided by feedback, and $B_1 = \text{diag}(b_p, b_q, b_r)$ is the inner loop bandwidth matrix.

Finally the control law for the fast states p, q, and r can be written in the form (17):

$$u = h_1^{-1}(x)[\dot{x}_{1d} - g_1(x)] \tag{17}$$

A necessary and sufficient condition for the existence of the control law (17) is nonsingularity of the matrix $h_1(x)$ over the entire domain of the state variables.

The control law for the slow states α, β, and ϕ was derived by manipulating the kinematic equations (4–6) and point mass equations of motion (7–9). We can write Eqs. (4–6) as

$$\dot{x}_2 = h_2(x) \cdot x_1 + g_2(x, \hat{z}) \tag{18}$$

where

$$h_2(x) = \begin{bmatrix} \sin\alpha & 0 & -\cos\alpha \\ -\tan\beta\cos\alpha & 1 & -\tan\beta\sin\alpha \\ 1 & 0 & 0 \end{bmatrix}$$

$$g_2(x, \hat{z}) = \begin{bmatrix} (Y + T_y\cos\beta - T_x\cos\alpha\sin\beta - T_z\sin\alpha\sin\beta)/(MV) \\ -(L - Mg\cos\gamma + T_x\sin\alpha - T_z\cos\alpha)/(MV\cos\beta) \\ 0 \end{bmatrix}$$

Inversion of Eq. (18) yields the control vector required to control the target's desired attitude rates:

$$x_{1c} = h_2^{-1}(x)[\dot{x}_{2d} - g_2(x, \hat{z})] \tag{19}$$

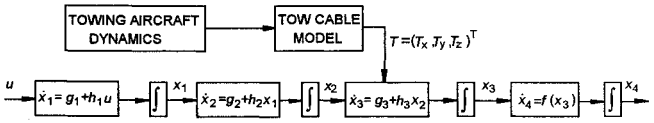

Fig. 3 Block diagram of the towed system dynamics.

Matrix $h_2(x)$ is right invertible for all β and all $\alpha \neq \pm\pi/2$. The vector of desired rates of the target attitudes is specified as

$$\dot{x}_{2d} = B_2[x_{2c} - x_2] \tag{20}$$

The vector x_2 in Eq. (20) is a combination of direct feedback measurement and estimates of the target attitude relative to the airflow, $B_2 = \text{diag}(b_\beta, b_\alpha, b_\phi)$ is the center loop bandwidth matrix.

Finally, to derive the control law for the vertical and horizontal flight-path angles, Eqs. (8) and (9) were employed. Using the small-angle approximations for the sine and cosine of α and β, and neglecting their products, these equations can be written in the following form:

$$\begin{bmatrix} \dot{\chi} \\ \dot{\gamma} \end{bmatrix} = h_3(x, \hat{z}) \begin{bmatrix} \beta \\ \alpha \end{bmatrix} + g_3(x, \hat{z}) \tag{21}$$

where

$$h_3(x, \hat{z}) = \begin{bmatrix} -\dfrac{T_x}{MV\cos\gamma} & 0 \\ 0 & \dfrac{T_x}{MV} \end{bmatrix}$$

$$g_3(x, \hat{z}) = \begin{bmatrix} \dfrac{Y + T_y}{MV\cos\gamma} \\ -\dfrac{g}{V}\cos\gamma + \dfrac{L - T_z}{MV} \end{bmatrix}$$

In fact, Eq. (21) is a combination of two independent equations, which can be inverted separately. The form of Eq. (21) was retained to fit into the general structure of the method. Desired rates of the flight-path angles are specified by linear feedback dynamics:

$$\begin{bmatrix} \dot{\chi} \\ \dot{\gamma} \end{bmatrix}_d = B_3 \begin{bmatrix} \chi_c - \chi \\ \gamma_c - \gamma \end{bmatrix} \tag{22}$$

where χ_c and γ_c are commanded flight-path angles produced by the maneuver generator, χ and γ are estimates of the states, and $B_3 = \text{diag}(b_\chi, b_\gamma)$ is outer loop bandwidth matrix.

The target considered is a vehicle of skid-to-turn type, using direct side force to turn with an X-configuration lifting surface geometry. To maximize the use of all four lifting surfaces for pitch and yaw control, the flight with constant roll angle $\phi_c = 0$ deg was commanded for all maneuvers considered in this study. Inverting Eq. (21) and using the zero roll angle command, the control vector that provides desired rates for the flight-path angles can be expressed as follows:

$$x_{2c} = \begin{bmatrix} \beta \\ \alpha \\ \phi \end{bmatrix}_c = \begin{bmatrix} h_3^{-1}(x, \hat{z}) \cdot \left\{ \begin{bmatrix} \dot{\chi} \\ \dot{\gamma} \end{bmatrix}_d - g_3(x, \hat{z}) \right\} \\ 0 \end{bmatrix} \tag{23}$$

Singularity of $h_3(x, \hat{z})$ can be prevented by establishing a lower bound on the T_x tension component. This bound has to be a positive constant (follows from physics of the system) with value dependent on the mass and aerodynamic drag of the target and the tow cable.

The block diagram of the complete control law is given in Fig. 4.

Simulation Results

For simulation purposes the geometry, mass, and aerodynamic parameters of the target were taken from Ref. 1 and represent the TRX-12 maneuverable towed vehicle developed by Hayes

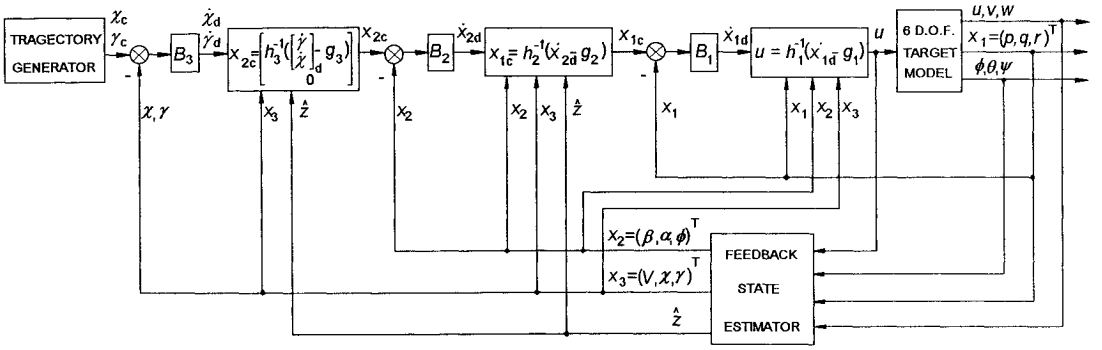

Fig. 4 Block diagram of nonlinear control law.

Table 1 Towed target and tow cable parameters

Parameter	Value
Mass M, kg	31
Reference area S, m^2	0.0324
Reference length $\bar{c}$, m	0.203
Wing span b[a], m	0.75
Inertia moments	
I_x, kg m^2	1.2558
$I_y = I_z$, kg m^2	10.563
$C_{L\alpha} = -C_{Y\beta}$	51.57
$C_{m\alpha} = -C_{n\beta}$	−70.69
$C_{mq} = C_{nr}$	−1173.87
$C_{L\delta_E} = C_{Y\delta_R}$	5.66
$C_{m\delta_E} = C_{n\delta_R}$	37.48
C_{lp}	−160.61
$C_{l\delta_A}$	15.2
C_{D0}[a]	0.4
Cable drag coefficients:	
Skin friction (tangential)	0.01
Crossflow (normal)	0.5
Cable mass per unit length, kg/m	0.03

[a]Assumed parameters.

International Targets. These parameters and cable-dependent data are given in Table 1.

The space envelope behind the aircraft where the towed system can be trimmed with zero roll angle, assuming that available elevator and rudder deflections are limited by ±20 deg, is shown in Fig. 5 for a towing speed of 100 m/s and cable lengths of 0.5 and 1 km.

In this study, the trajectories to be followed by the target were selected inside the boundary area depicted in Fig. 5, and thus the problem of command control limiting is not discussed here.

The effect of the feedback gain values on the closed-loop system's tracking performance and level of control activity was studied by simulating a rapid maneuver of the towed target. As expected, increasing feedback gains in all three loops leads to better tracking. Unacceptably low performance was observed when the outer loop gains b_χ and b_γ were below 3.0 s^{-1}. The level of control activity required increases with an increase of the elements of the B_2 and B_3 gain matrices of the center and the outer loops (slow dynamics). However, an increase of the gains of the inner loop (fast dynamics) leads to a lower level of control activity. A numerical instability in the simulation occurred when the elements of the B_1 matrix were in the region below 1.5 s^{-1}. To obtain satisfactory tracking in both horizontal and vertical directions, greater values of gains are required for the channels corresponding to longitudinal states than those corresponding to lateral states.

To compromise between tracking performance and control expenditure, the following values of the gains were selected for further simulations: B_1 = diag(4.0, 6.0, 3.5), B_2 = diag(5, 7.5, 4), and B_3 = diag(3.5, 5).

Guidance and Station Keeping

The NI control law's maneuvering properties were compared with those of the guidance algorithm suggested in Ref. 1. Any trajectory of the target (with restrictions from the cable in mind) can be described by means of the required displacements in the $Oxyz$ reference frame with its origin in the trim position of the target's center of mass with controls locked. Horizontal displacement of the target in the positive y direction by 100 m in 10 s is considered here as example of a lateral maneuver. For the NI control law the trajectory is generated simply by specifying coordinates of the required new position of the target's center of mass. Figures 6a and 6b show time histories of a priori estimated elevator and rudder deflections generated by the algorithm[1] and produced by the NI control law. The navigation quality of the NI control law (obtained using extensive feedback and an increased computational load) is illustrated, in Figs. 6c and 6a, by the time histories of the target's coordinates y and z in accomplishing the maneuver. As use of a station-keeping autopilot is assumed in Ref. 1, the trajectory obtained with the guidance algorithm only (dotted lines) may not serve for a complete performance comparison. It can be seen that the NI control system performs a station-keeping function as the cable continues oscillating after the target has reached the required position.

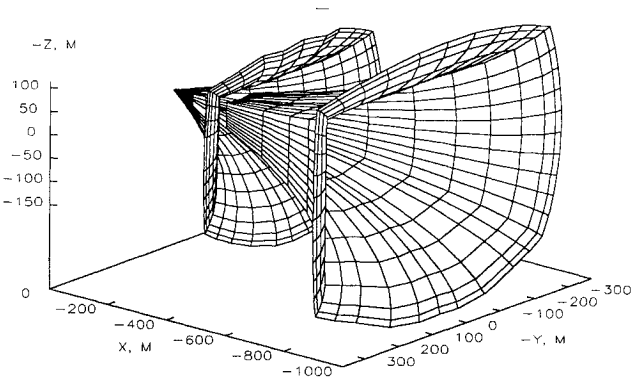

Fig. 5 Space envelope behind the aircraft where the towed system can be trimmed.

A spiral of radius R around the trim position is considered as an example of three-dimensional trajectory to be flown by the target. Time dependence of the center of mass coordinates for the stable motion along this trajectory can be approximately described as follows:

$$y(t) = R\cos(t_0 + \omega t)$$
$$z(t) = R\sin(t_0 + \omega t) \tag{24}$$

where ω is rotation frequency, and t_0 is initial time of stable rotation.

From differentiation of Eq. (24) it follows that linear velocities $\dot{y}_d$ and $\dot{z}_d$, which should be produced by the target to track the spiral, are also sinusoidal functions with amplitude proportional to the product of the radius R and frequency ω.

For the straight level flight of the towing aircraft (which was assumed in this study) the relation between displacement of the target center of mass in the $Oxyz$ reference frame and magnitude and direction of the velocity vector can be obtained using Eqs. (11)

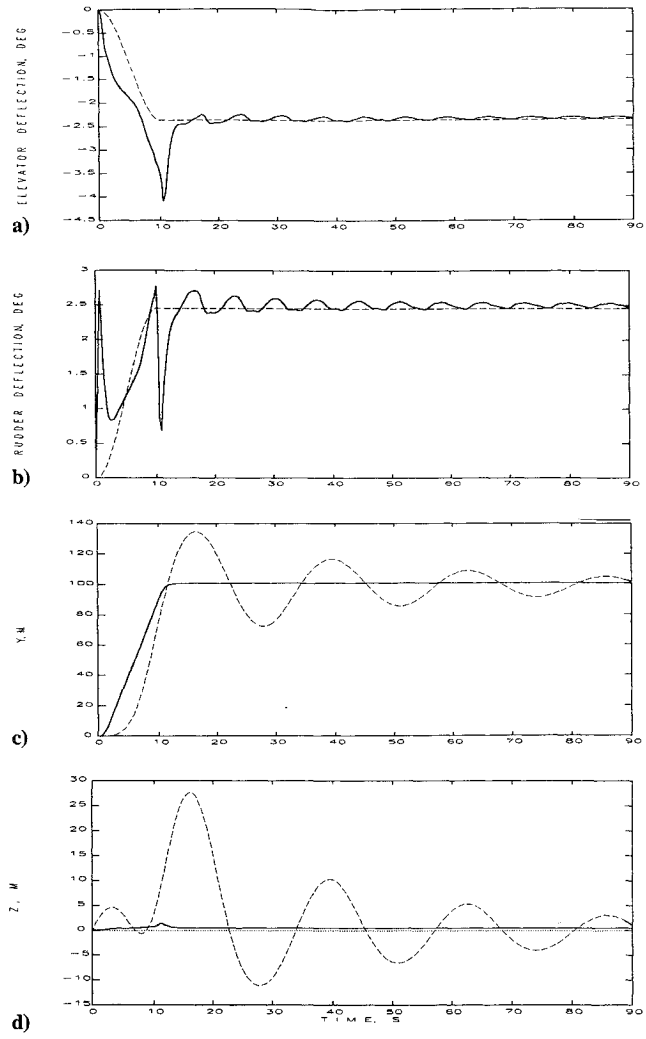

Fig. 6 Maneuver out of vertical plane with guidance algorithm[1] (dashed lines) and NI control law (solid lines).

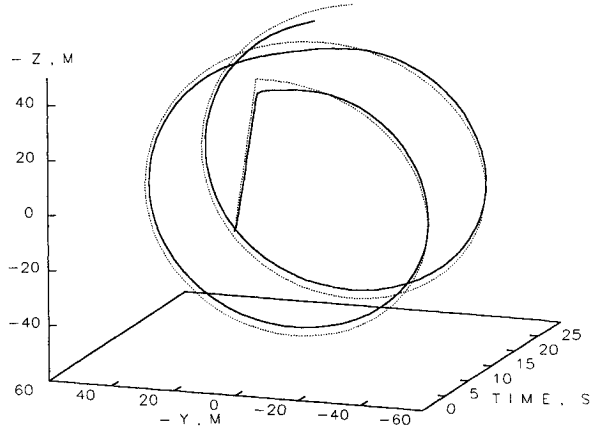

Fig. 7 Towed target trajectory (solid line) in tracking a commanded spiral (R = 50 m and ω = 0.1 Hz) (dotted line).

and (12). Simplified by small-angle approximations these relations become

$$\dot{y} = V_x; \qquad \dot{z} = V_y \tag{25}$$

Now using Eq. (25) the commanded flight-path angles necessary to track the desired trajectory can be determined by

$$\gamma_c = (\dot{y}_d/V); \qquad \chi_c = (\dot{z}_d/V) \tag{26}$$

Equations (26) were employed to generate three-dimensional maneuvers to be flown by the target.

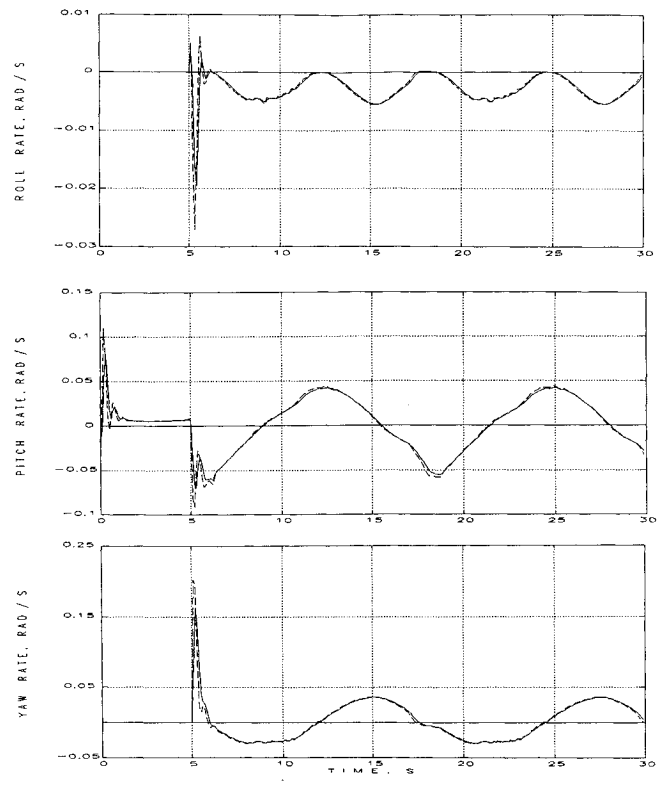

Fig. 8 Inner loop (fast dynamics) commanded signals (dashed lines) and states (solid lines).

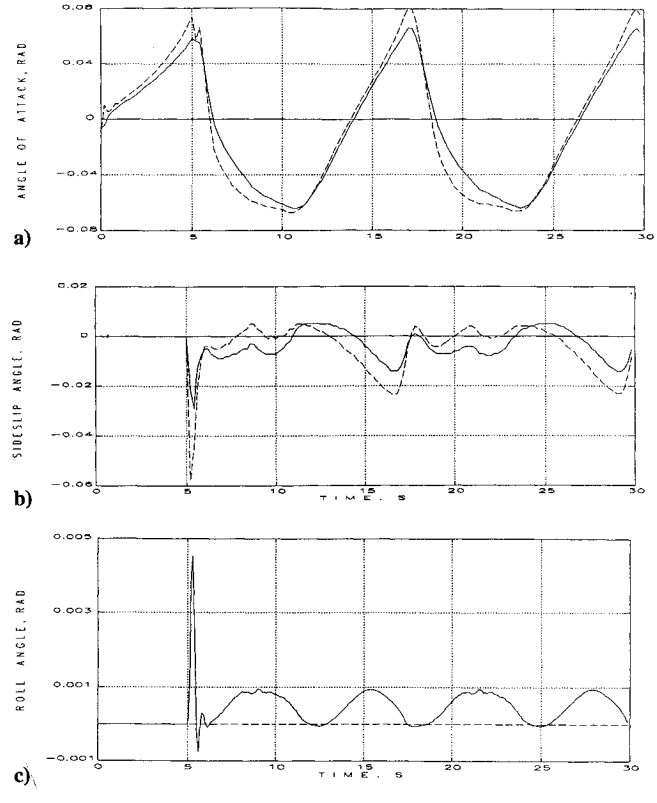

Fig. 9 Center loop (slow dynamics) commanded signals and states.

It should be mentioned that trajectories where, at any point, both T_y and T_z body axis components of the tension force are simultaneously approaching zero (or a predetermined small quantity) should be avoided, as it results in the tow cable aligning itself with the target longitudinal axis and disturbs the motion of the target.

Figure 7 shows the trajectory produced by the target (solid line) with NI control law tracking a commanded spiral of radius R = 50 m and rotation frequency ω = 0.1 Hz (dotted line). The spiral

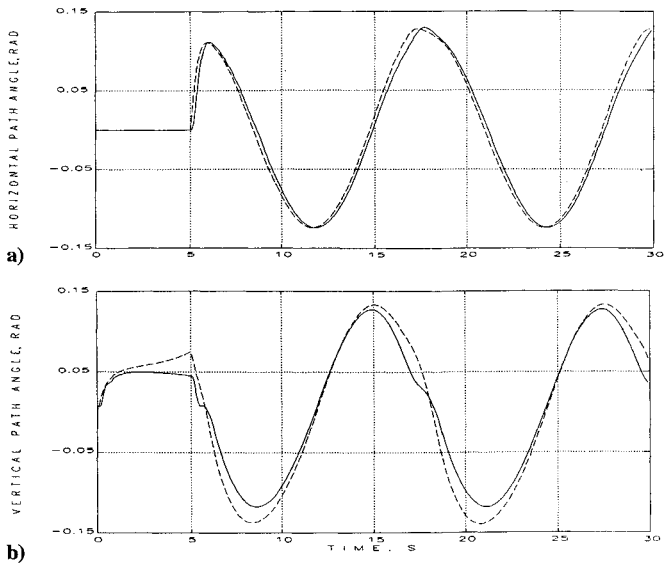

Fig. 10 Outer loop commanded signals and states.

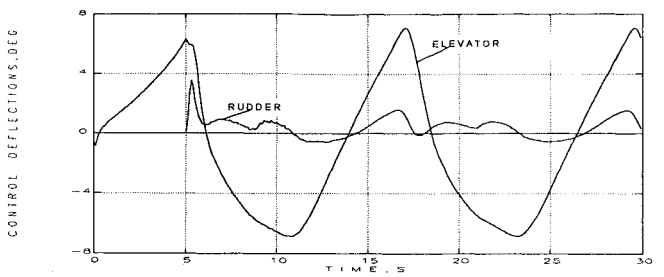

Fig. 11 Time histories of the control deflections along the spiral trajectory.

is generated after the target is guided into the point 50 m above its trim position in 5 s.

Generated command signals and tracking properties of the NI control laws, with the feedback gains as defined previously, are illustrated in Figs. 8–10 for inner, center, and outer loops, respectively. Figure 11 shows time histories of elevator and rudder commands produced by the NI control law to track the trajectory of spiral form.

The behavior of the fast and slow dynamic variables (Figs. 8 and 9, respectively) in tracking of the commanded signals validates the system decomposition into the faster and slower modes. Figure 9c shows that the roll angle remains within 0.3 deg along the trajectory and thus conforms to the assumption made in obtaining Eqs. (4–9).

Time histories of the horizontal and vertical flight-path angles are shown in Figs. 10a and 10b, respectively (solid lines). Commanded signals produced by the maneuver generator are plotted in dashed lines.

Simulation results have shown that distribution of the forces determines different levels of control effort required to move the towed system in the vertical direction than for horizontal motion. This fact is illustrated well in Fig. 11 for the trajectory of spiral form.

Conclusions

The design of a control system that enables an aerial towed body to follow trajectories involving rapid maneuvering is a difficult and inherently nonlinear problem. To solve it, a control system design technique based on inversion of nonlinear dynamic and kinematic equations of motion has been applied. The cable tension force has been taken into account. A conventional set of feedback parameters was assumed, and the procedure used for estimation of the aerodynamic and tension forces acting on the target and states unavailable directly by measurement has been described.

The developed control law provides guidance in rapid three-dimensional maneuvers of the target and performs a station-keeping function when steady positioning is required.

Although a linear aerodynamic model of the target was used in this design, the nonlinear inversion method is able to make use of nonlinear aerodynamic data.

Acknowledgments

This work was supported in part by the Australian Defence Science and Technology Organisation. The authors would like to thank the reviewers for their constructive comments that helped to clarify the presentation.

References

[1]Cochran, J. E., Innocenti, M., No, T. S., and Thukral, A., "Dynamics and Control of Manoeuverable Towed Flight Vehicles," *Journal of Guidance, Control, and Dynamics*, Vol. 15, No. 5, 1992, pp. 1245–1251.

[2]Singh, S. N., and Rugh, W. J., "Decoupling in a Class of Nonlinear Systems by State Variable Feedback," *Journal of Dynamic Systems, Measurement, and Control*, Dec. 1972, pp. 323–327.

[3]Asseo, S. J., "Decoupling of a Class of Nonlinear Systems and Its Application to an Aircraft Control Problem," *Journal of Aircraft*, Vol. 10, No. 12, 1973, pp. 739–747.

[4]Lane, S. H., and Stengel R. F., "Flight Control Design Using Nonlinear Inverse Dynamics," *Automatica*, Vol. 24, No. 4, pp. 471–483.

[5]Bugajski, D. J., and Enns, D. F., "Nonlinear Control Law with Application to High Angle-of-Attack Flight," *Journal of Guidance, Control, and Dynamics*, Vol. 15, No. 3, 1992, pp. 761–767.

[6]Chow, J. H., and Kokotovic, P. V., "Two-Time-Scale Feedback Design of a Class of Nonlinear System," *IEEE Transactions on Automatic Control*, Vol. AC-23, No. 3, 1978.

[7]Snell, S. A., Enns, D. F., and Garrard, W. L., "Nonlinear Inversion Flight Control for a Supermanoeuverable Aircraft," *Journal of Guidance, Control, and Dynamics*, Vol. 15, No. 4, 1992, pp. 976–984.

[8]Noriaki Nakagava, and Akira Obata, "Longitudinal Stability Analysis of Aerial-Towed Systems," *Journal of Aircraft*, Vol. 29, No. 6, 1992, pp. 978–985.

[9]Sanders, J. V., "A Three Dimensional Dynamic Analysis of a Towed System," *Ocean Engineering*, Vol. 9, No. 5, 1982, pp. 483–499.

[10]Dreyer, T. P., and Murray D. M., "The Numerical Solution of the Pre-Elimination Models of Cable Configurations," *Journal of Computational and Applied Mathematics*, No. 10, 1984, pp. 81–91.

[11]May, R. L., and Connell, H. J., "Towed Systems Modelling Study," Royal Melbourne Inst. of Technology, Dept. of Mathematics, Rept. 10, Melbourne, Victoria, Australia, 1988.

[12]Chapman, D. A., "Cable-Body Aerodynamic (Underwater) Simulator," Program Manual, School of Engineering, Univ. of Bath, Oct. 1983.

[13]Ochi, Y., and Kanai, K., "Design of Restructurable Flight Control Systems Using Feedback Linearisation," *Journal of Guidance, Control, and Dynamics*, Vol. 14, No. 5, 1991, pp. 903–911.